JOURNAL OF GEOPHYSICAL RESEARCH, VOL. 115, C02004, doi:10.1029/2009JC005601, 2010

Evaluation of a 3-D hydrodynamic model and atmospheric forecast forcing using observations in Lake Ontario

Anning Huang,[1,2] Yerubandi R. Rao,[2] and Youyu Lu[3]

Received 25 June 2009; revised 2 October 2009; accepted 5 October 2009; published 3 February 2010.

[1] Six-month observations of surface meteorology, water temperature, and currents in Lake Ontario are used to evaluate a high-resolution, three-dimensional hydrodynamic model and the forecasted forcing from a regional version of the Canadian operational global environmental multiscale (GEM) model. The hydrodynamic model is based on the Princeton Ocean Model (POM). Driven by both the observed and modeled surface wind stress and the surface net heat fluxes (SNHF), POM is able to reproduce the observed variations of the lake surface temperature (LST) and vertical stratification conditions at the seasonal and synoptic time scales. The model also has skill in simulating the temporal and vertical variation of currents. The patterns of the simulated horizontal distributions of the LST and lake circulation are consistent with the observed climatology. Model sensitivity experiments reveal that the differences between the simulations using observed and model forcing are mainly due to the difference in wind stress instead of the SNHF. Comparison with meteorological observations suggests that GEM has good accuracy in simulating the SNHF but overestimates the wind. Model sensitivity experiments further revealed that errors in the SNHF have significant impact on simulations of water temperature in the surface and near-surface layers, whereas errors in wind stress cause significant changes of water temperature in the thermocline.

Citation: Huang, A., Y. R. Rao, and Y. Lu (2010), Evaluation of a 3-D hydrodynamic model and atmospheric forecast forcing using observations in Lake Ontario, *J. Geophys. Res.*, *115*, C02004, doi:10.1029/2009JC005601.

1. Introduction

[2] The Laurentian Great Lakes extend from the southern edge of the permafrost line to the southern extent of the Wisconsin glaciation (between 40°N and 50°N). They form the largest group of freshwater lakes in the world. With horizontal scales of hundreds of kilometers, depth scales of 100 m, the Laurentian Great Lakes are large enough to include some physical phenomena associated with the coastal oceans and are sometimes referred to as inland seas. The Great Lakes system has a total surface area of approximately 245,000 km^2 and a total water volume of approximately 22,700 km^3. Such a huge water body has an important impact on determining regional weather and climate [*Anyah and Semazzi*, 2004]. Compared to land surface, the lakes have very different albedo, heat capacity, and roughness, and are large sources of moisture for the lower atmosphere. Many studies [e.g., *Scott and Huff*, 1996; *Liu and Moore*, 2004] show that those Great Lakes that are not frozen during late autumn and early winter can generate large amounts of snowfall on their leeward coast. This lake effect is associated with the stimulation of atmospheric convection and cloud formation when cold air masses pass across the relatively warmer lake surface. However, when the lake water is relatively colder compared to nearby land areas and air (e.g., during upwelling events in summer), thermal stability of the lower atmosphere can occur over and near the air-water interface. The convective boundary layer is suppressed over the lakes, resulting in decrease of cloudiness in the downwind [*Segal et al.*, 1997]. On the other hand, atmospheric conditions, such as air temperature, heat transfer between air-lake interface, precipitation, evaporation, and lake surface winds also have significant impacts on the thermal structure, currents, and water level in large lakes [*Gibson et al.*, 2006].

[3] Studies have shown that inclusion of air-lake interactions leads to improved performance of climate models. For example, idealized lakes are included in general circulation models (GCMs) [e.g., *Bonan*, 1995; *Lofgren*, 1997] and one-dimensional lake models are included in regional climate models (RCMs) [e.g., *Hostetler et al.*, 1993; *Bates et al.*, 1995]. However, these simple lake models only account for the vertical heat transfer by eddy diffusion and convective mixing without treating advective heat transfer between neighboring lake points in the horizontal. This kind of air-lake coupling may be justified for small lakes, but it is too simple to represent complex lake-air interactions over large lakes because of the significant large spatial variability in the surface temperatures. Recently, a few attempts have been made to couple three-dimensional lake models with RCMs [*Song et al.*, 2004; *Long et al.*,

[1]School of Atmospheric Sciences, Nanjing University, Nanjing, China.
[2]NWRI, Water Science and Technology Directorate, Environment Canada, Burlington, Ontario, Canada.
[3]Department of Fisheries and Oceans, Bedford Institute of Oceanography, Dartmouth, Nova Scotia, Canada.

0148-0227/10/2009JC005601$09.00

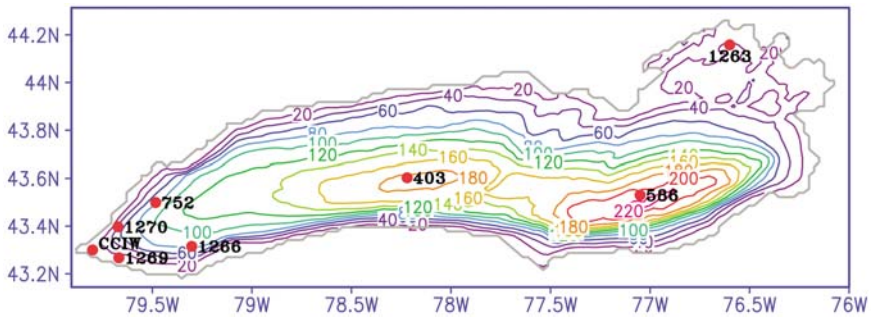

Figure 1. Bathymetry of Lake Ontario in the model domain (in meters) and the locations of meteorological, water temperature, and acoustic Doppler current profiler moorings.

2007]. Their results show that fully coupled air-lake regional climate model systems provide reasonable temporal evolution of lake surface temperature (LST) and heat transfer at the air-lake interface in large lakes, allowing important feedbacks between the atmosphere, adjacent land, and the lakes at fine scales. However, the lake simulations were not systematically validated with observations in most of these studies. Such validations are necessary before fully coupling the three-dimensional lake models with atmospheric models for predicting regional weather, climate, and air-lake interactions over the Great Lakes region.

[4] Currently, the lake ice component of the operational atmospheric system in the Canadian Meteorological Centre (CMC) is treated as static, with the water surface temperature values being specified according to the analysis of observations for determining heat fluxes into the atmosphere at the surface of the lake. *Pellerin et al.* [2004] showed improved weather forecasts over the Gulf of St. Lawrence and adjacent coastal areas by using a fully coupled atmosphere–ocean ice system in a case study involving rapid ice motion. Encouraged by these results, a fully coupled regional air-lake atmospheric modeling system over the Great Lakes region is planned. Before the coupled system is completed, it is important to assess the accuracy of the surface fluxes from the current CMC operational atmospheric model, namely, the global environmental multiscale (GEM) model. In this study, the GEM forcing is used to drive a 3-D hydrodynamic model of Lake Ontario. The results of this simulation are directly compared with observations in the lake, as well as with the results of another simulation using the observed atmospheric forcing interpolated onto the model grids. The comparison enables the evaluation of both the lake hydrodynamic model and the GEM model forcing. Further, additional model sensitivity experiments are conducted to test the dependence of lake simulation on forcing accuracy.

[5] In section 2, the limnological condition and observational data in Lake Ontario are introduced. The lake hydrodynamic model and forcing data are described in section 3. The model experiments and analysis of the model results are presented in section 4. A summary of conclusions is provided in section 5.

2. Lake Ontario Application

[6] Lake Ontario extends from 43.1°N to 44.3°N and 80°W to 76°W and has a surface area of 19,529 km^2 and a volume of 1637 km^3. Its mean depth is 86 m with a maximum depth of 245 m located in the southeast region (Figure 1). Since Lake Ontario is located downstream of the other members of the Great Lakes, it is impacted by human activities occurring throughout the Great Lakes region. The downwind side of Lake Ontario is known to have high snowfalls due to lake effects [*Dewey*, 1979]. Modeling of large lake systems requires high-quality data with sufficient temporal and spatial resolutions. Compared to most other lakes, Lake Ontario has a wealth of archived meteorological and hydrographic data [*Saylor et al.*, 1981]. Furthermore, the lake has a rich history of studies using theoretical and numerical models [*Simons*, 1974, 1975]. These studies described the basic characteristics of circulation and temperature. In 2006, an intensive field investigation was undertaken to gain new information about meteorology, water temperature, and currents in the lake. The data collected during spring and summer period offer the opportunity to validate the lake hydrodynamic model and atmospheric model forcing.

[7] The field measurement program was undertaken by Environment Canada (EC) in both the nearshore and middle of Lake Ontario during 15 April to early October 2006. Four meteorological buoys (stations CCIW, 403, 586, and 1263, as shown in Figure 1) provided observations of solar radiation, incoming longwave radiation, surface air and water temperatures, wind speed and direction, atmospheric pressure, and relative humidity. The atmospheric variables were measured approximately 4 m above the lake level. Wind speed observations were adjusted to a common reference height of 10 m by using a logarithmic profile. Hourly vertical profiles of water temperature were obtained from four thermistor strings (stations 1266, 752, 403, and 586, as shown in Figure 1). Three broadband acoustic Doppler current profilers were deployed at three stations (1266, 1269, and 1270, as shown in Figure 1) and provided continuous measurements of velocity profiles. In addition, the LST averaged over Lake Ontario derived from satellite remote sensing is available. We obtain the daily time series in 2006 from the CoastWatch data set (ftp://coastwatch.glerl.noaa.gov/glsea/avgtemps/2006/glsea-temps2006.dat) of the U.S. Great Lakes Environmental Research Laboratory (GLERL).

3. Lake Hydrodynamic Model and Forcing Data

3.1. Lake Hydrodynamic Model

[8] The lake hydrodynamic model is based on the latest version of the Princeton Ocean Model (POM) which was originally developed in the 1980s [*Blumberg and Mellor*,

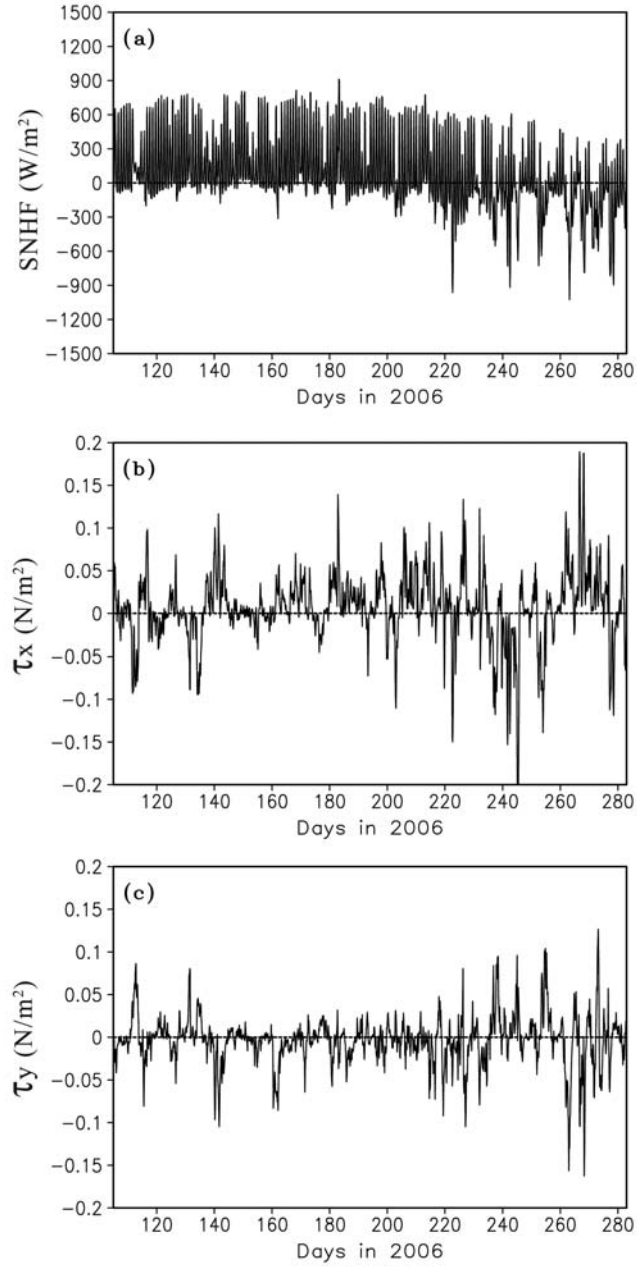

Figure 2. Time series of (a) the observed 3-hourly mean SNHF and (b, c) two components of wind stress at station 403.

1987]. It is a three-dimensional, nonlinear, free surface, and primitive equation coastal ocean model. POM solves the conservation equations of heat, mass, and momentum on staggered grids using the finite difference method. It uses a terrain following vertical coordinate system (i.e., sigma coordinates) scaled on the water column depth. The vertical mixing coefficients are determined by a second-moment turbulence closure submodel. POM adopts a mode splitting technique to solve the barotropic mode for the free surface and the baroclinic mode for the full three-dimensional temperature, turbulence, and currents. Detailed description of the model is available in the Users' Guide of POM [*Mellor*, 2004]. POM has been applied to simulate the surface temperature distributions in Lake Erie [*Kuan et al.*, 1994] and the seasonal and interannual variability of circulation and thermal structure in Lake Michigan [*Beletsky et al.*, 2006]. Recently, POM has also been used as the lake model component in regional coupled air-lake climate model systems [*Song et al.*, 2004; *Long et al.*, 2007].

[9] The POM for Lake Ontario has 31 vertical sigma levels and a uniform horizontal grid size of 2 km. Vertical levels are spaced more closely in the upper 30 m of water and near the bottom to better resolve the surface and bottom boundary layers and the thermocline. The centers of the sigma levels are located at −0.0005, −0.0035, −0.013, −0.030, −0.053, −0.073, −0.089, −0.10, −0.12, −0.135, −0.151, −0.165, −0.181, −0.196, −0.212, −0.227, −0.242, −0.269, −0.331, −0.419, −0.506, −0.594, −0.681, −0.769, −0.856, −0.91, −0.93, −0.95, −0.97, and −0.99. The model has two open boundaries (i.e., the south and east open boundaries). At the southern open boundary, the discharge from Niagara River to Lake Ontario is set to a constant of 5600 m^3/s. At the eastern boundary, the outflows from Lake Ontario into St. Lawrence River are split into the north exit (2850 m^3/s) and the south exit (2750 m^3/s). The river temperatures are simply taken from the nearest grid points in the lake.

[10] At the lake surface, POM is forced by wind stress and surface net heat flux (SNHF). The east-west and north-south components of the wind stress are given by

$$\tau_x = \rho_a C_d |\vec{V}| u$$
$$\tau_x = \rho_a C_d |\vec{V}| v, \quad (1)$$

where $|\vec{V}|$ is the wind speed, u and v are the wind speed components in the east-west and north-south directions, ρ_a is air density, and C_d is a drag coefficient set to a constant of 1.3×10^{-3}. The SNHF is given by $Q = S + \mathrm{NL} + \mathrm{SH} + \mathrm{LH}$, where S is the solar radiation; NL is the net long wave radiation; LH is the latent heat flux, and SH is the sensible heat flux. We note that the modeled LST is used in the computation of LH and SH during model integration. The different heat flux components are calculated using bulk formulae of *Schertzer* [1987] and defined as positive when they tend to heat the lake.

3.2. Forcing Data

[11] The meteorological observations at four stations (CCIW, 403, 586, and 1263) are used as inputs for deriving atmospheric forcing at 3-hourly intervals. Figure 2 shows the time series of the SNHF and wind stress at station 403. Both the SNHF and wind stress have significant synoptic and seasonal variations; and the SNHF also has obvious diurnal variation. Table 1 gives the correlation coefficients

Table 1. Correlation of the Observed SNHF and Wind Stress Between Station 403 and Each of the Stations CCIW, 586, and 1263

	Station CCIW	Station 586	Station 1263
SNHF	0.82	0.94	0.92
τ_x	0.74	0.86	0.78
τ_y	0.54	0.82	0.56

Table 2. Summary of POM Experiments

	Heat Flux	Wind Stress
OF	observation	observation
MF	GEM	GEM
MF1	GEM (four stations)	GEM (four stations)
SEN1	observation	GEM
SEN2	GEM	observation
SNHFP	observation × 1.1	observation
SNHFN	observation × 0.9	Observation
WINDP	observation	observation × 1.21
WINDN	observation	observation × 0.81

between each of the stations CCIW, 586, and 1263 and the station 403 for each of the flux components. Among the four stations, the SNHF has a high level of consistency while the wind stress has evident differences. Because of the spatial variability of the observed atmospheric fields at the four stations, they are interpolated onto the model grids using a distance weighing method defined as $f = \sum_i (f_i/\alpha_i)/\sum_i (1/\alpha_i)$, where α_i is the distance between the model grids and the ith station and f_i is the value of an observed variable at the ith station.

[12] The modeled meteorological forcing data are taken from the 0–24 h forecasts of a regional version of GEM with a grid spacing of 15 km [*Mailhot et al.*, 2006]. The GEM-forcing fields are at 3 h interval. A bilinear interpolation method is used to map the GEM-forcing fields onto the POM grids. The observed and modeled forcing will be compared later in section 4.3.

4. Numerical Experiments

[13] A total of nine numerical experiments with different surface forcing (Table 2) are carried out. The salinity is set to a constant value of 0.2 parts per thousand to reflect the freshwater condition of the lake [*Sheng and Rao*, 2006]. Considering the vertical temperature gradients are very small in early spring, the initial temperature at each model grid is simply initialized with the average LST observed at four stations (stations CCIW, 403, 586, and 1263) on 15 April 2006. All the nine model cases start on 15 April and end on 10 October of 2006. Before carrying out the model simulations, we have done a set of model runs driven by the observed meteorological forcing in order to optimize the main parameters in POM. Reasonable thermal structure and currents in Lake Ontario are obtained by using a multiplier value of $C = 0.1$ for horizontal diffusion in the Smagorinsky eddy parameterization [*Mellor and Blumberg*, 1985] and *Jerlov*'s [1976] type I of optical categories.

4.1. Validation of Modeled Variations of Temperature and Current

[14] The observed forcing (OF) experiment is treated as a base case, in which the model is driven by the spatially

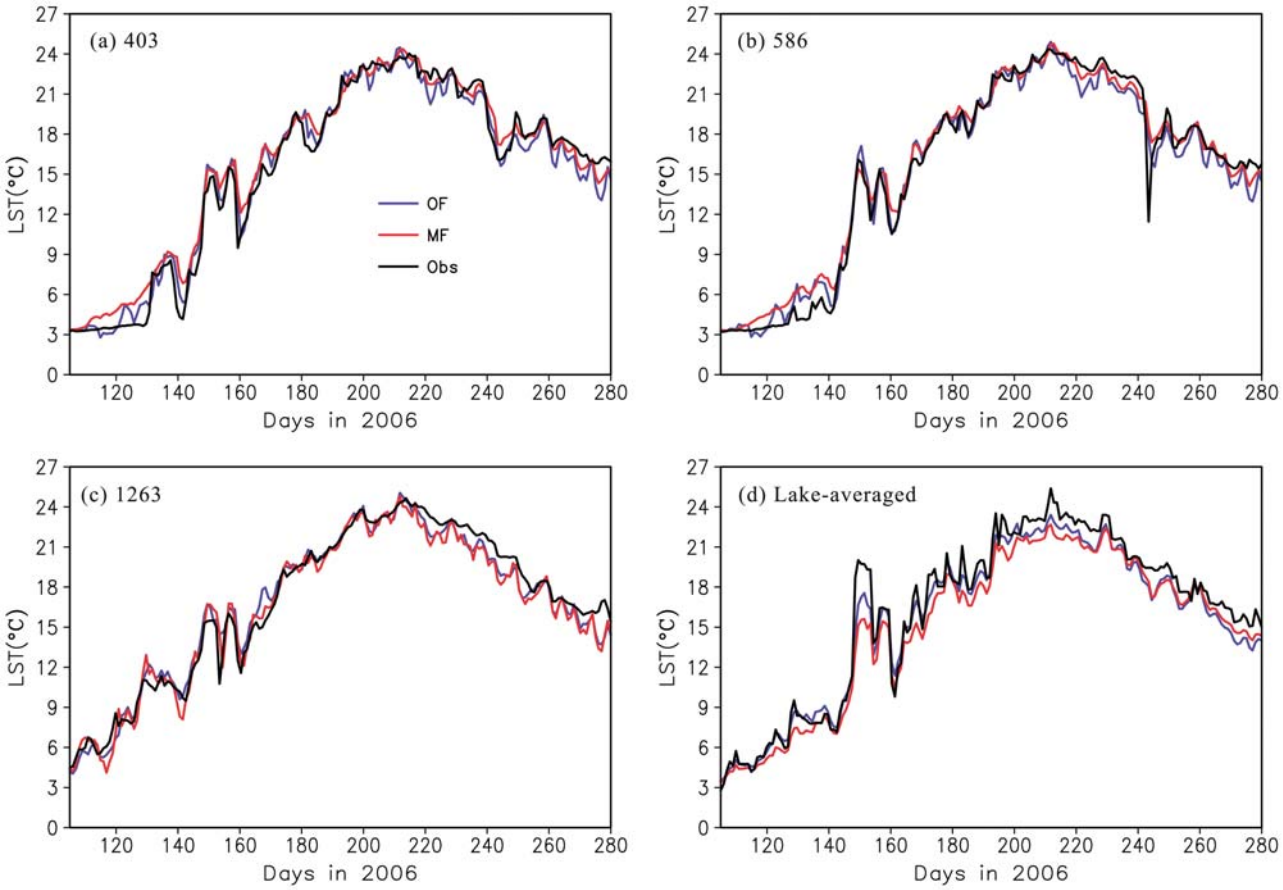

Figure 3. Time series of the observed and modeled lake surface temperature at stations (a) 403, (b) 586, (c) 1263 and (d) averaged over the whole lake.

Table 3. LST Root-Mean-Square-Error and Average Percentage Difference Between the Observation and Simulations From OF and MF During 15 April to 10 October 2006

	OF		MF	
Sites	RMSE (°C)	Average Percentage Difference (%)	RMSE (°C)	Average Percentage Difference (%)
403	1.03	−0.64	1.23	3.09
586	1.01	−0.88	1.09	2.01
1263	0.95	−0.89	1.03	−2.32
Lake averaged	1.09	−1.83	1.43	−4.36

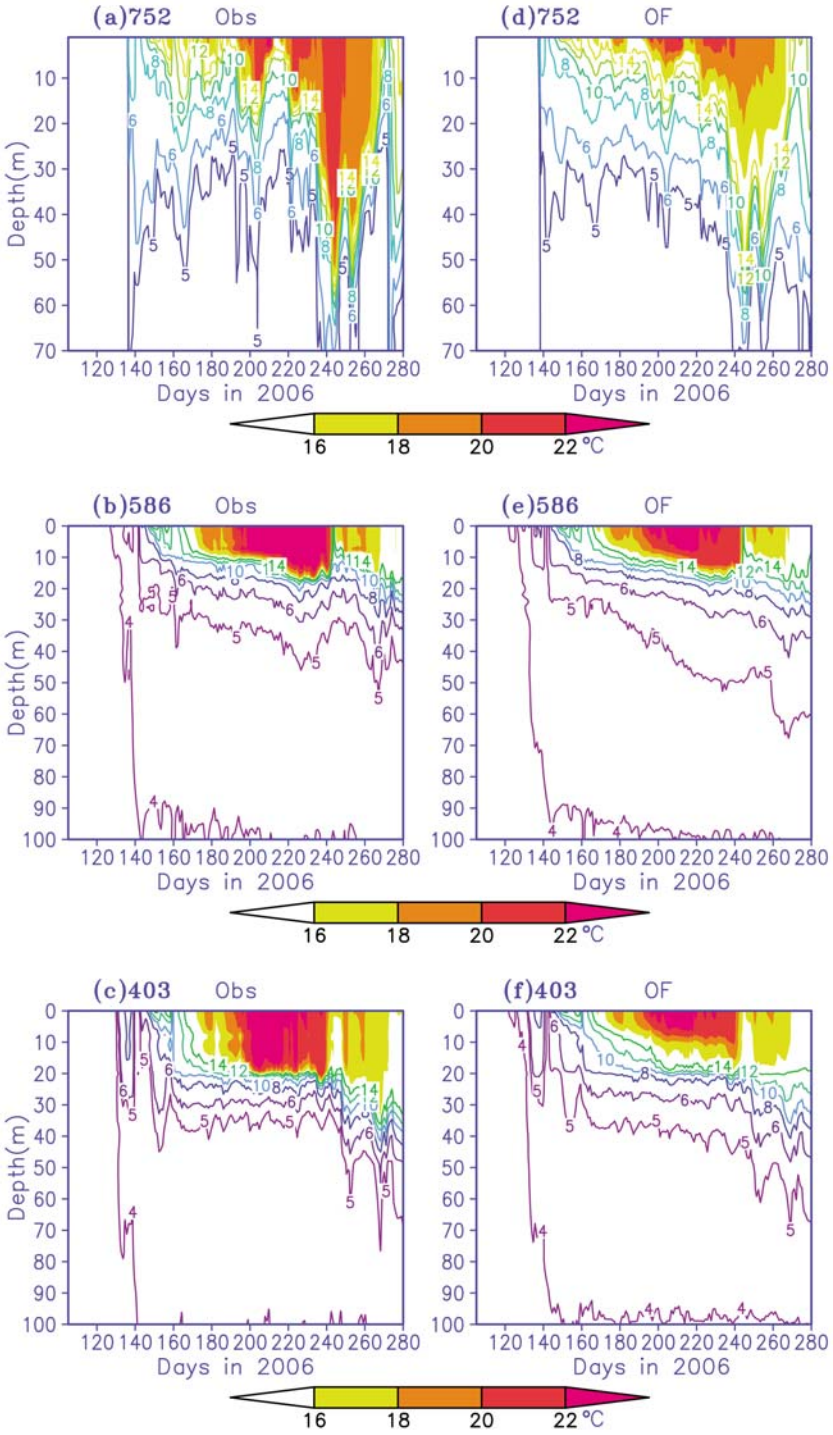

Figure 4. Time-depth distributions of water temperature from (a–c) observations and (d–f) the model results in OF experiment at stations 752, 586, and 403. Unit is °C.

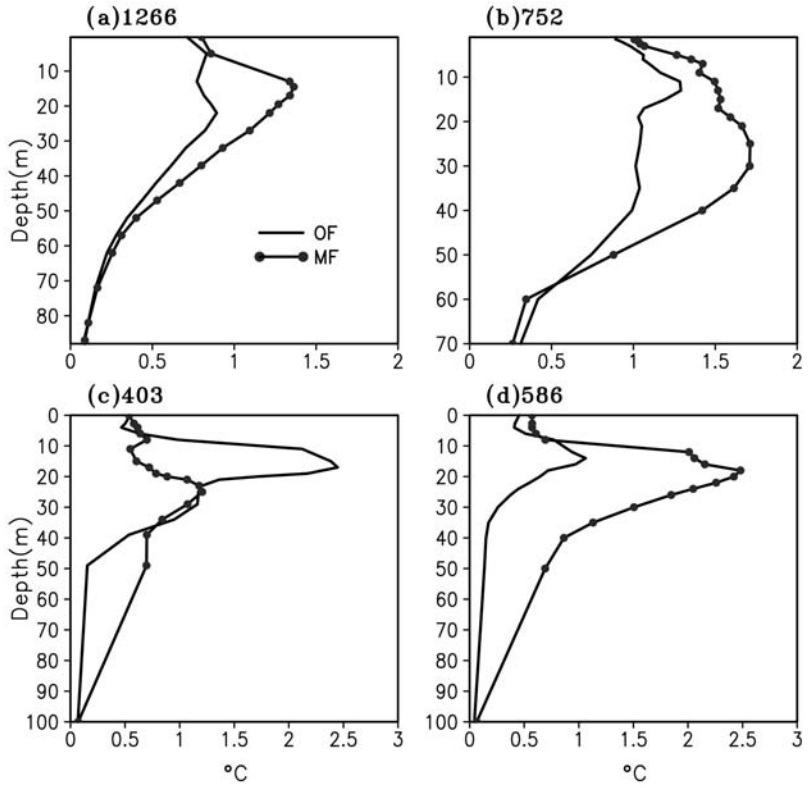

Figure 5. The vertical profile of the RMSE between observed and modeled temperature at stations (a) 1266, (b) 752, (c) 403, and (d) 586. Unit is °C.

interpolated wind stress and heat fluxes from observations at four stations. The model forcing (MF) experiment is driven by forcing from GEM forecast. Figure 3 shows the time series of LST from observations and from the OF and MF experiments at stations 403, 586, and 1263, and also averaged over the whole lake. Note that the observed lake-averaged LST is derived from the GLERL data set. Both model experiments well reproduce the observed seasonal variation of LST, i.e., the warming from spring to summer and cooling from summer to fall. Significant variations at synoptic time scales, e.g., a rapid lakewide warming and subsequent strong oscillations in spring, are also well simulated. The model also captures a rapid cooling and subsequent warming in fall at station 586, although underestimates the magnitude of the changes. The simulations have a noticeable cold bias during summer to fall at station 1263. It also appears that the simulations overestimate the magnitudes of synoptic variations during summer and fall at all stations and the whole lake.

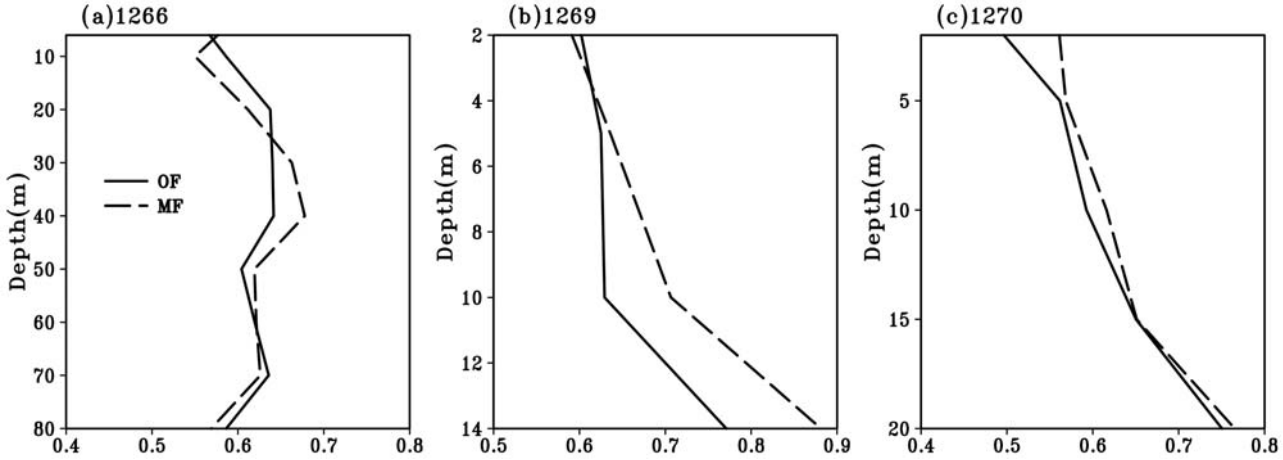

Figure 6. The vertical profile of normalized Fourier norms between simulated and observed currents at stations (a) 1266, (b) 1269, and (c) 1270.

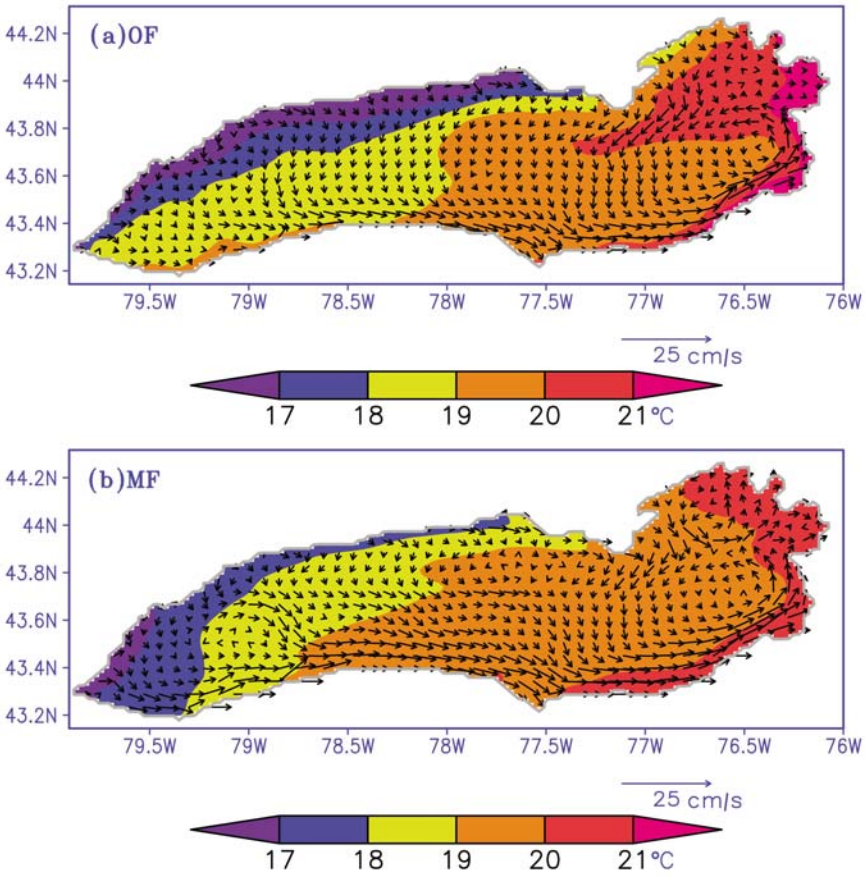

Figure 7. The simulated summer mean near-surface (1–2 m) currents (vector) and temperature (shaded) distributions in Lake Ontario from the (a) OF and (b) MF experiments.

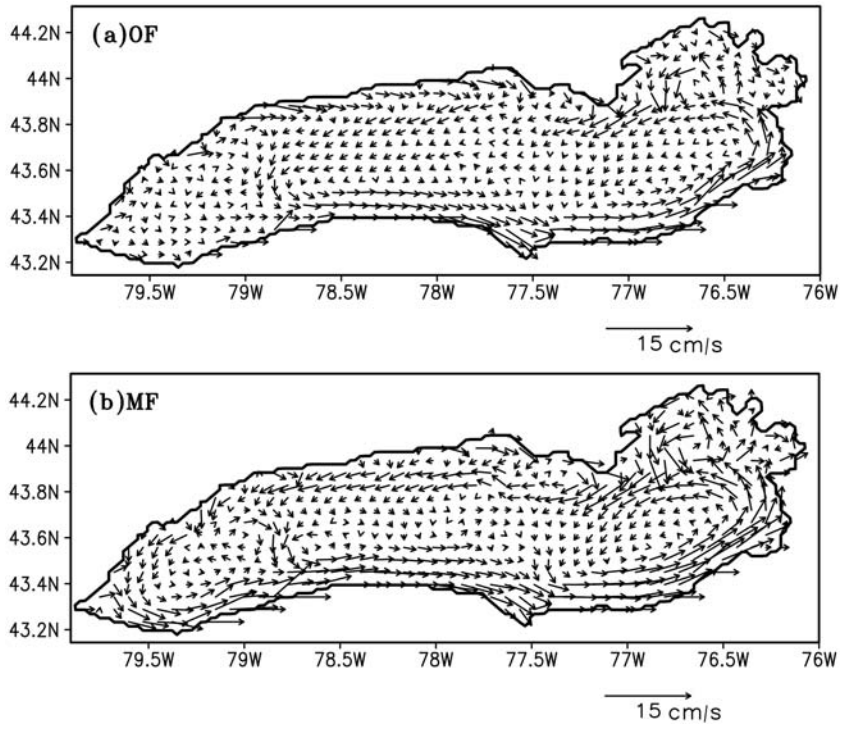

Figure 8. The simulated summer mean depth-averaged currents distributions in Lake Ontario from the (a) OF and (b) MF experiments.

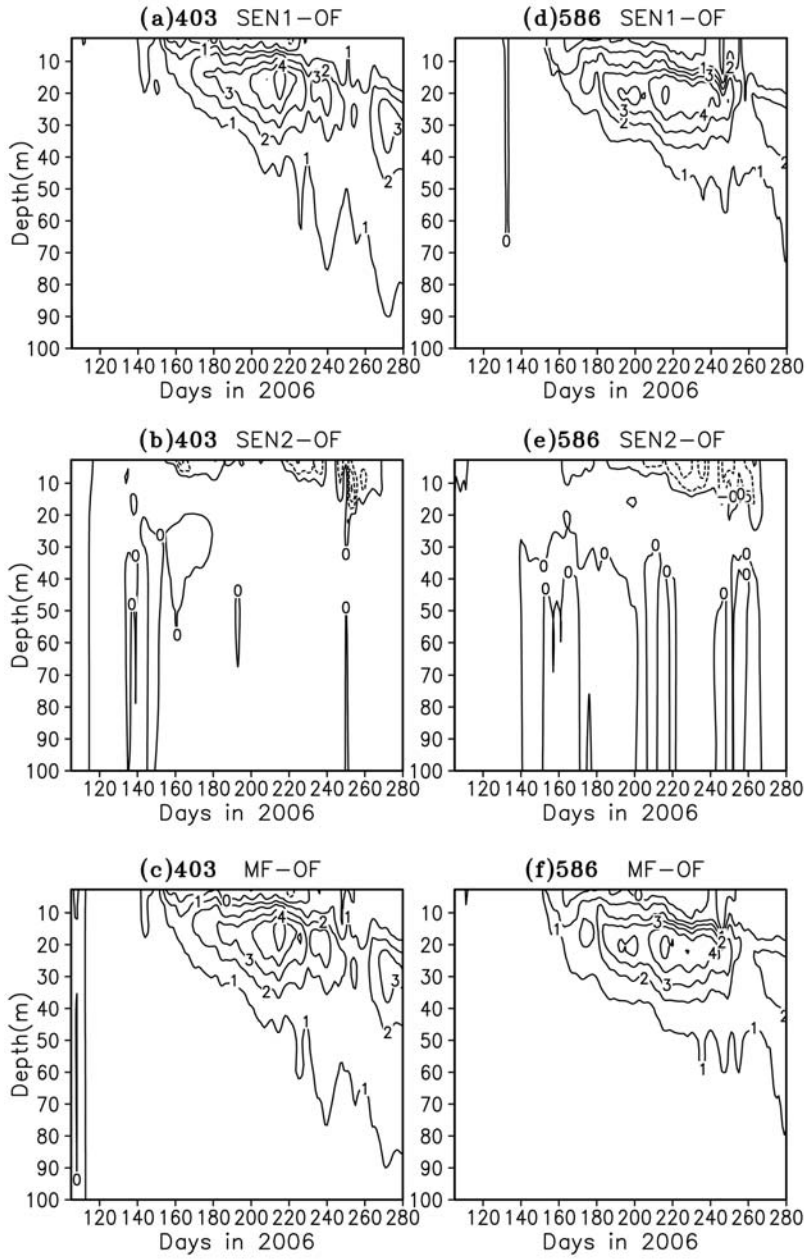

Figure 9. Time-depth distributions of the differences in temperature between each of the (a, d) SEN1, (b, e) SEN2, and (c, f) MF experiments and the OF experiment at stations 403 and 586. Unit is °C.

[15] Two metrics are used to quantify the errors of the modeled water temperature. The first is the root-mean-square error (RMSE) defined by

$$\mathrm{RMSE} = \left(\frac{1}{M} \sum_{i=1}^{M} \left(f_i^{\mathrm{m}} - f_i^{\mathrm{o}} \right)^2 \right)^{1/2}, \tag{2}$$

where f_i^{m} and f_i^{o} are modeled and observed water temperature for sample case i (out of M sample cases), respectively. The second metric is the average percentage difference (P_d) between the observation and simulation defined by

$$P_d = \left(\frac{1}{M} \sum_{i=1}^{M} \left[\left(f_i^{\mathrm{m}} - f_i^{\mathrm{o}} \right) / f_i^{\mathrm{o}} \times 100\% \right] \right). \tag{3}$$

As shown in Table 3, the RMSE ranges from 0.95°C to 1.09°C for the simulation with the observed forcing and from 1.03°C to 1.43°C for the simulation with GEM forcing. The ranges of model errors are similar with that of earlier POM simulations in Lake Michigan [*Beletsky et al.*, 2006]. The average percentage difference of LST is smaller for the OF simulation than the MF simulation. The slightly higher error of the simulation with GEM forcing is expected because GEM treats the lake as static, therefore does not account for temperature variations in the mixed layer in the lake.

[16] To further examine the model skill in simulating the vertical thermal structure of temperature, the time-depth distributions of the simulated temperatures are compared with the observations made at different thermistor stations. According to observations (Figures 4a–4c), in summer the

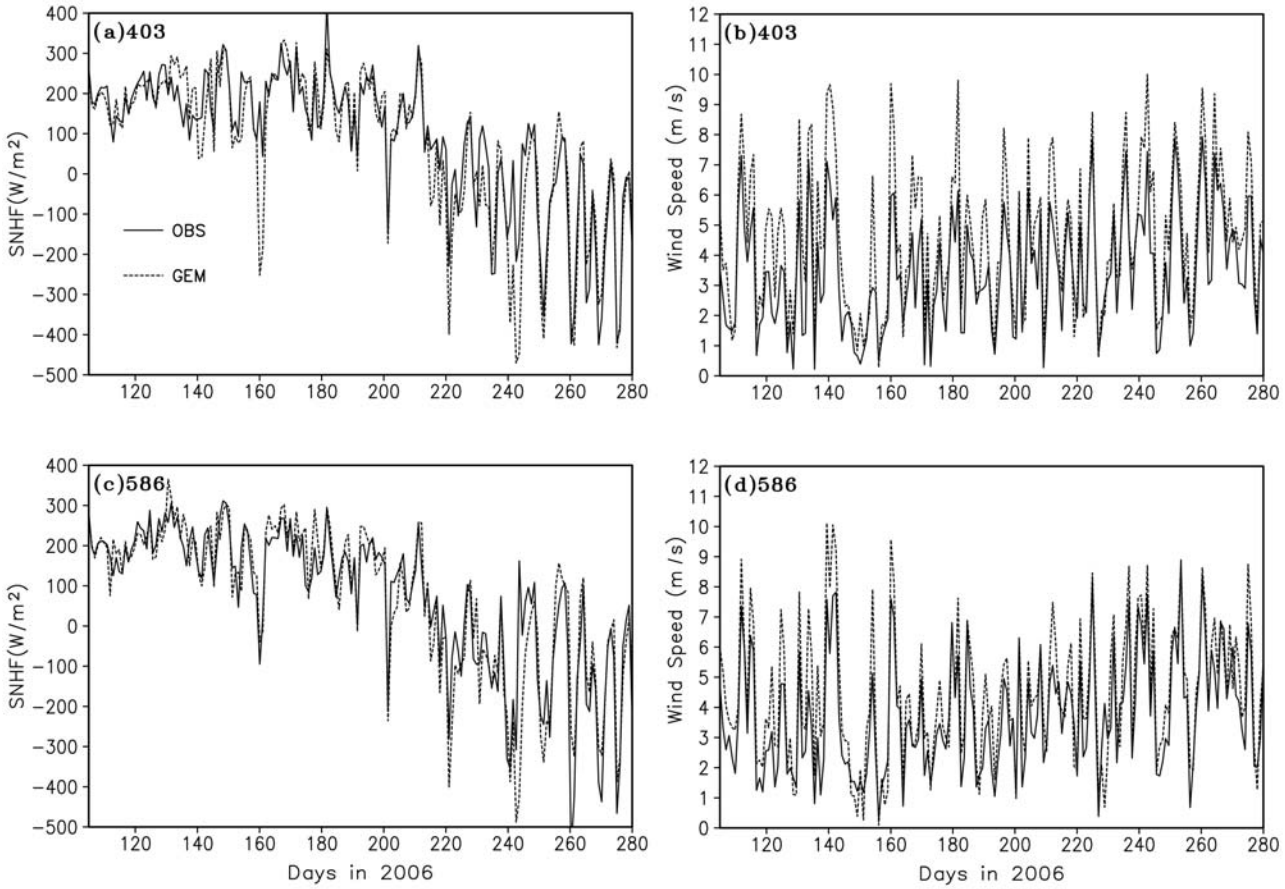

Figure 10. Time series of the observed and GEM forecast of surface net heat flux and wind speed at stations (a, b) 403 and (c, d) 586.

thermocline in shallow area (station 752) is deeper than those in the deep water region (stations 403 and 586). In the deeper waters at stations 403 and 586 with water depth more than 180 m, the lake is stratified with a warm surface layer of about 20 m thick. Below this layer a sharp thermocline is present from day 150 to 280. Temperatures at depth below 50 m are almost always less than 5°C. However, in the shallower region at station 752 the thermocline depth varied significantly corresponding to changes in wind. During an easterly wind episode in early September, the thermocline at this station dipped below 40 m because of downwelling along the north shore. Surface heat losses and increased vertical mixing associated with strong winds result in deepening of the thermocline from late September until the water column is again mixed from top to bottom in fall.

[17] The time-depth changes in water temperature from the OF experiment are presented in Figures 4d–4f. The dominant features of the evolving thermal stratification of the water column are reasonably well captured by POM. In the coastal area (station 752) the model is able to reproduce the upwelling and downwelling events in the water column. Early studies [e.g., *Beletsky and Schwab*, 2001] show that the model mixed layers tend to be slightly shallower than observation. This is not the case in the present solutions; however, the thermocline is somewhat diffuse.

[18] The model errors in simulating the vertical thermal structure are quantified using RMSE between the simulated and observed temperatures at stations 1266, 752, 403, and 586 (Figure 5). In general, the OF experiment using the observed forcing produced smaller RMSE values than the MF experiment in the mixed layer and the thermocline, except in the lower mixed layer and thermocline at station 403. The higher RMSE values are generally located in the lower mixed layer and thermocline region, where strong high-frequency temperature oscillations induced by internal waves are not simulated by the model.

[19] The flows in the lake are highly variable in time and space. The misfit between modeled and observed currents is quantified by

$$Fn = \left(\frac{1}{M}\sum_{t=\Delta t}^{M\Delta t}|V_m - V_o|^2\right)^{1/2} \Big/ \left(\frac{1}{M}\sum_{t=\Delta t}^{M\Delta t}|V_o|^2\right)^{1/2}, \quad (4)$$

where V_m and V_o are modeled and observed currents, respectively. Fn is a normalized Fourier norm of the time series of modeled and observed currents [*Beletsky et al.*, 2006]. It can also be thought of as the relative percentage of variance in the observed currents that is unexplained by the model. The smaller Fn, the better the model results fit the observations. For the OF and MF experiments, Fn ranges from 0.5 to 0.9 at the three sites for the daily mean currents simulated (Figure 6). Compared to the offshore station (1266), predictions at nearshore stations generally deteriorated toward

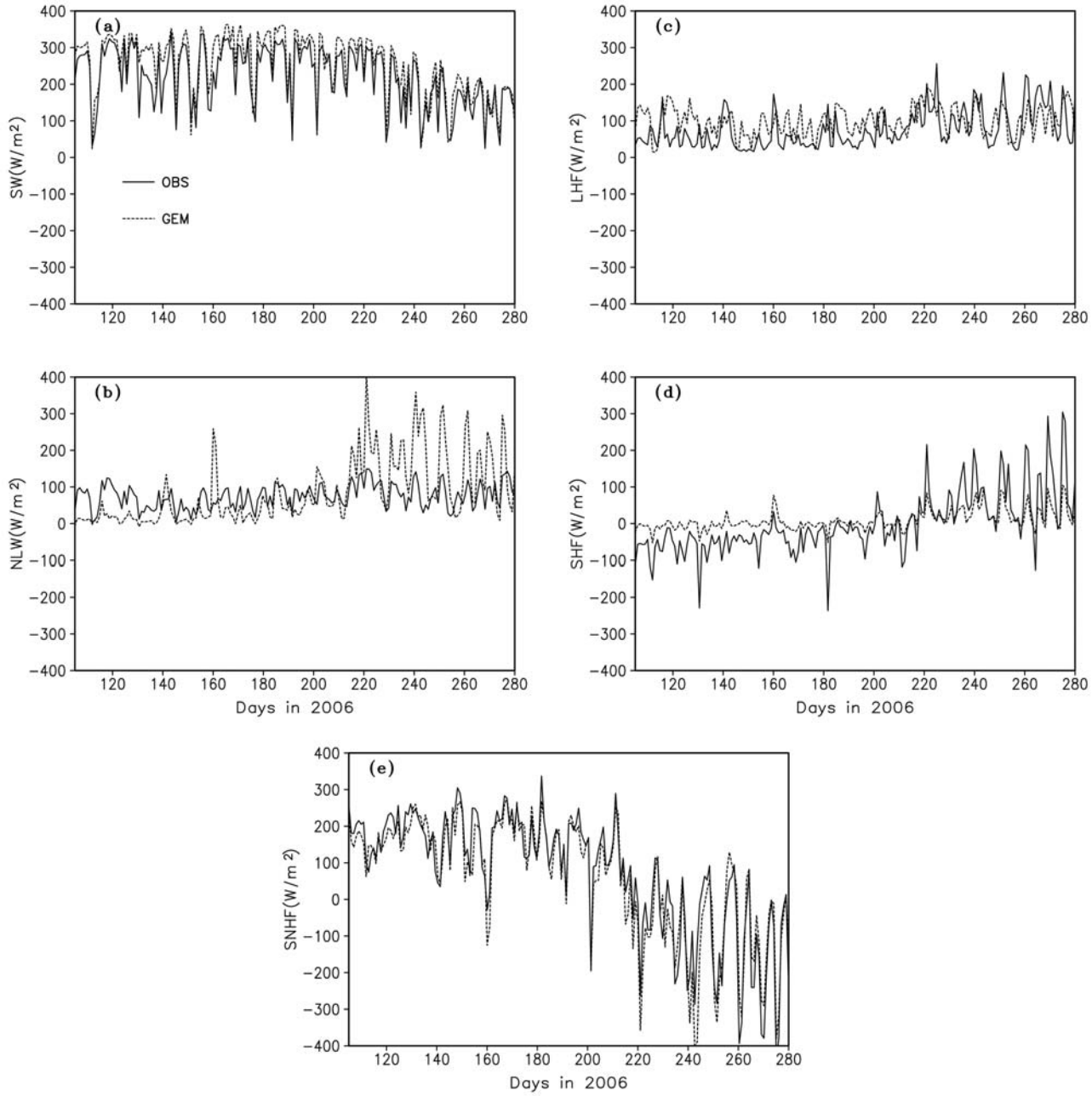

Figure 11. Time series of the GEM modeled and observed surface heat fluxes averaged over the four stations (stations CCIW, 403, 586, and 1263): (a) shortwave radiation, (b) net longwave radiation, (c) latent heat flux, (d) sensible heat flux, and (e) surface net heat flux.

the bottom. The *Fn* values still are comparable to other studies [*Beletsky et al.*, 2006]. The currents produced by both observed and model forcing are only slightly different from each other, indicating that the model winds may be adequate for predicting surface currents in the lake.

4.2. Horizontal Distributions of Seasonal Mean Surface Temperature and Currents

[20] The horizontal distributions of the near-surface temperature are linked to changes in air-lake heat flux and the redistribution of heat by currents. Figure 7 shows the modeled summer (June–August) mean near-surface (1–2 m) temperature and currents simulated by the OF and MF experiments. The spatial distributions from the two experiments are comparable. The near-surface temperature increases from west to east. The near-surface temperature is less than 18°C in the northwestern part of the lake, and it is over 20°C in the east. This spatial distribution is mainly a consequence of the prevailing mean eastward (westerly) wind in summer over the lake, which causes upwelling along the north shore and downwelling along the southeastern shore. The modeled spatial pattern of the near-surface temperature is consistent with the observed climatology [*Saulesleja*, 1986]. The simulated near-surface currents show a lakewide cyclonic (counterclockwise) circulation

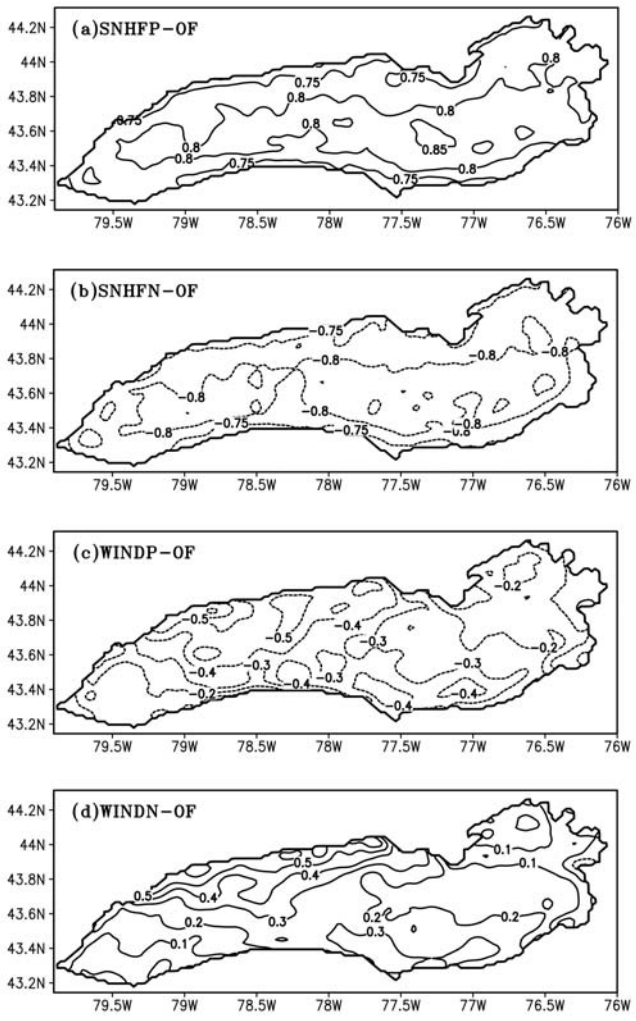

Figure 12. The spatial distributions of the differences in LST between each of the four sensitivity experiments and the OF experiment averaged over the whole simulation period. Unit is °C.

with stronger flow along the southern coast than along the northern coast.

[21] Figure 8 shows the summer mean depth-averaged currents simulated by the OF and MF experiments. The circulation simulated using the GEM forcing is stronger than that simulated using the observed forcing. From both experiments, the depth-averaged currents show lakewide cyclonic circulation with similar pattern in the near-surface circulation. The MF experiment obtains westward flow in the north part of the lake similar with the flow pattern documented by early studies [*Simons*, 1974; *Rao and Murthy*, 2001]. The strong eastward currents along the south shore obtained from both experiments are similar with that documented in early studies as well [e.g., *Saylor et al.*, 1981; *Beletsky et al.*, 1999].

4.3. Sensitivity of Model Results to Meteorological Forcing

[22] The differences between the OF and MF experiments, as discussed in previous sections, can be caused by differences in wind stress or surface heat fluxes, or both. One issue of concern is how the lake model performance is affected by the difference in spatial resolutions between the observed and model forcing. To check this, we extract the time series of GEM forcing at the locations of the four meteorological observational stations. The time series of forcing are then spatially interpolated to POM grids following the same procedure used for observed forcing. The experiment of using this four-station only GEM forcing is named MF1. The results from the MF and MF1 experiments have a high level of consistency. In terms of LST, the spatial and temporal correlations are over 0.96; the average percentage differences are below 1%; and the RMSE values are comparable. The above comparison confirms that the differences between OF and MF experiments cannot be attributed to the differences in spatial resolutions between the two types of forcing.

[23] To further understand the dependence of the POM simulations to each forcing component, the SEN1 and SEN2 experiments are carried out. SEN1 is driven by the observed SNHF and GEM winds. SEN2 is driven by the GEM SNHF and observed winds (see Table 2). Figure 9 shows the time-depth distributions of the differences in temperature between each of the MF, SEN1, SEN2 experiments, and the OF experiment at two stations. The differences between the SEN1 and OF experiments (Figures 9a and 9d) reflect the impacts of changes in wind stress. It is shown that changes in wind stress cause significant changes in the vertical thermal structure in the thermocline region. In comparison, changes in the SNHF (Figures 9b and 9e, the differences between the SEN2 and OF experiments) mainly cause discrepancy in the upper mixed layer (less than 10 m depth). Figures 9c and 9f show the differences between the MF and OF experiments. The differences are significant from below 5 m to the depth of 40 m (in the lower mixed layer and the thermocline). Clearly, the differences between the MF and OF experiments in water temperature can mainly be accounted for by differences in wind stress instead of the SNHF.

[24] The time variations of the SNHF and wind speeds from GEM are compared with observations at stations 403 and 586 in Figure 10. For each variable at each station, the correlations between observation and simulation are over 0.9. The averaged percentage differences in wind speeds between the GEM results and observation are 27.5% and 21.9% at stations 403 and 586, respectively. However, the averaged percentage differences of SNHF between the GEM simulation and observation are −5.3% and −2.5% at stations 403 and 586, respectively. GEM simulates the SNHF with a high accuracy despite the treatment of the lakes as static. Figure 11 further shows the different components of the heat fluxes averaged over the four stations, from observations and GEM. Compared with the observed time series, GEM slightly overestimates the solar radiation during mid-April to early October (Figure 11a); underestimates (overestimates) the net longwave radiation before (after) July (Figure 11b); and overestimates (underestimates) the latent and sensible heat fluxes before (after) early August (Figures 11c and 11d). In general, the SNHF from GEM and observations are quite close (Figure 11e). Although GEM overestimated the net longwave radiation after day 220, it underestimated the sensible heat flux

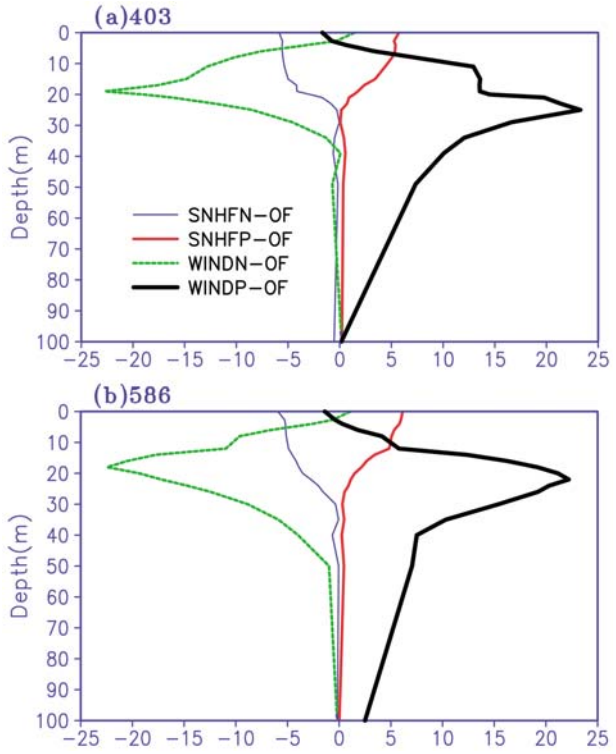

Figure 13. Vertical profile of the average percentage differences in water temperature during the stratified period between each of the four sensitivity experiments and the OF experiment at stations (a) 403 and (b) 586.

during this period, which resulted in relatively small errors in the SNHF.

[25] The above analyses suggest that the GEM forecasts have better accuracy in the SNHF compared to wind speed. A further insight of the model sensitivity can be assessed by a set of additional runs with different forcing components of similar degree of errors. To achieve this, we perform four additional experiments, each by changing the wind speed (not wind direction) or the SNHF by ±10% compared with the observation. These experiments are named as SNHFP (+10% difference in SNHF), SNHFN (−10% difference in SNHF), WINDP (+10% difference in wind speed, or +21% in wind stress) and WINDN (−10% difference in wind speed, or −19% in wind stress), respectively. Figure 12 shows the spatial distributions of the differences in LST between each of these experiments with the OF experiment. As shown in Figures 12a and 12b, the lakewide LST increases (decreases) by about 0.8°C when the SNHF increases (decreases) by 10%. By comparison, increasing (decreasing) the wind speed by 10% results in decreasing (increasing) of the LST by 0.2°C–0.5°C (Figures 12c and 12d).

[26] Figure 13 shows the vertical profile of the mean percentage differences in temperature during the stratified period (June to September 2006) between each of the four additional experiments and the OF experiment at two stations. Clearly, the temperature in the upper layer up to 10 m depth increases (decreases) by about 5% when the SNHF increases (decreases) by 10%. The temperature in the thermocline increases (decreases) by 20–25% while the changes in LST are only by 1–2% when the wind speed increases (decreases) by 10%. The above analyses reveal that the 10% in SNHF leads to moderate errors in temperature in the surface and near-surface layers in the lake. On the other hand, 10% error in the wind speed causes insignificant errors in the LST, whereas significant errors in temperature in the lower mixed layer and thermocline during the stratified period.

5. Conclusions

[27] Meteorological and limnological data were collected during an intensive field program in Lake Ontario. This comprehensive data set is used to validate a high-resolution lake hydrodynamic model and the forcing from a regional configuration of the Canadian atmospheric forecasting model GEM. The approach taken is to force POM with the observed and the modeled surface fluxes, and comparing both model results with observed lake temperature and currents. Both the OF and MF experiments show considerable skills reproducing the observed time variations of the LST and the vertical stratification conditions at synoptic and seasonal time scales. The quantification using two metrics (the RMSE and the average percentage difference) reveals that the OF experiment has higher accuracy than the MF experiment. This is different from the results of *Beletsky et al.* [2003] which showed that forcing from an atmospheric mesoscale model (MM5) appeared to be superior to observations. One possible reason is that the GEM has a lower resolution (15 km) compared with that of MM5 (6 km). In terms of the time variations of the currents, the OF and MF experiments possess similar accuracy; the values of the normalized Fourier norm are comparable to previous studies. The modeled horizontal distributions of the seasonal mean water temperature and circulation are consistent with the observed climatology.

[28] Model sensitivity experiments (SEN1 and SEN2) reveal that the differences between the solutions of the OF and MF simulations are mainly due to the differences in wind stress instead of the SNHF. Compared with the observed surface fluxes, the GEM forcing has a good accuracy in the SNHF but significantly overestimates the wind stress. The additional four sensitivity experiments reveal the different response of POM to errors in the SNHF and wind stress. Increasing (decreasing) the SNHF causes increasing (decreasing) in water temperature that is confined in the surface and near-surface layers. By comparison, increasing (decreasing) the wind stress results in decreasing (increasing) in the lake surface temperature. However, the most significant impacts of errors in wind stress are found in the thermocline.

[29] In summary, the validation exercise presented in this study suggests that the high-resolution 3-D hydrodynamic model based on POM and the GEM forecast forcing are both of good quality for simulating the synoptic and seasonal variations of water temperature and currents in Lake Ontario. The present study is focused on the ice-free season. An ice component is needed for simulating the lake state in winter, although the ice condition in Lake Ontario is light compared with other members of the Great Lakes. At least for the ice-free seasons, the results of the present study are encouraging for further development of the coupled air-lake modeling system for the Great Lakes region.

[30] **Acknowledgments.** The authors wish to thank Jun Zhao for her help in processing GEM model output. Frank Bryan and two anonymous reviewers provided constructive comments that helped to improve the original manuscript.

References

Anyah, R. O., and F. H. M. Semazzi (2004), Simulation of the sensitivity of Lake Victoria basin climate to lake surface temperatures, *Theor. Appl. Climatol.*, *79*, 55–69, doi:10.1007/s00704-004-0057-4.

Bates, G. T., F. Giorgi, and S. W. Hostetler (1995), Toward the simulation of the effects of the Great Lakes on regional climate, *Mon. Weather Rev.*, *121*, 1373–1387.

Beletsky, D., and D. J. Schwab (2001), Modeling circulation and thermal structure in Lake Michigan: Annual cycle and interannual variability, *J. Geophys. Res.*, *106*, 19,745–19,771.

Beletsky, D., J. H. Saylor, and D. J. Schwab (1999), Mean circulation in the Great Lakes, *J. Great Lakes Res.*, *25*, 78–93.

Beletsky, D., D. J. Schwab, R. P. Roebber, M. J. Mccormick, G. S. Miller, and J. H. Saylor (2003), Modeling wind-driven circulation during the March 1 998 sediment resuspension event in Lake Michigan, *J. Geophys. Res.*, *108*(C2), 3038, doi:10.1029/2001JC001159.

Beletsky, D., D. J. Schwab, and M. McCormick (2006), Modeling the 1998–2003 summer circulation and thermal structure in Lake Michigan, *J. Geophys. Res.*, *111*, C10010, doi:10.1029/2005JC003222.

Blumberg, A. F., and G. L. Mellor (1987), A description of a three dimensional coastal ocean circulation model, in *Three Dimensional Ocean Models*, *Coastal Estuarine Sci. Ser.*, vol. 5, edited by N. S. Heaps, pp. 1–16, AGU, Washington, D. C.

Bonan, G. B. (1995), Sensitivity of a GCM simulation to inclusion of inland water surfaces, *J. Clim.*, *8*, 2691–2704.

Dewey, K. F. (1979), An objective forecast method developed for Lake Ontario induced snowfall systems, *J. Appl. Meteorol.*, *18*, 787–793.

Gibson, J. J., T. D. Prowseand, and D. L. Peters (2006), Hydroclimatic controls on water balance and water level variability in Great Slave Lake, *Hydrol. Processes*, *20*, 4155–4172.

Hostetler, S. W., G. T. Bates, and F. Giorgi (1993), Interactive coupling of a lake thermal model with a regional climate model, *J. Geophys. Res.*, *98*, 5045–5057.

Jerlov, N. G. (1976), *Marine Optics*, 231 pp.Elsevier Sci., New York.

Kuan, C., K. W. Bedford, and D. J. Schwab (1994), A preliminary credibility analysis of the Lake Erie portion of the Great Lakes forecasting system for springtime heating conditions, in *Quantitative Skill Assessment for Coastal Ocean Models*, *Coastal Estuarine Stud.*, vol. 47, edited by D. R. Lynch and A. M. Davies, pp. 397–423, AGU, Washington, D. C.

Liu, A. Q., and G. W. K. Moore (2004), Lake-effect snowstorms over southern Ontario, Canada, and their associated synoptic-scale environment, *Mon. Weather Rev.*, *132*, 2595–2609.

Lofgren, B. M. (1997), Simulated effects of idealized Laurentian Great Lakes on regional and large-scale climate, *J. Clim.*, *10*, 2847–2858.

Long, Z., W. Perrie, J. Gyakum, D. Caya, and R. Laprise (2007), Northern lake impacts on local seasonal climate, *J. Hydrometeorol.*, *8*, 881–896, doi:10.1175/JHM591.1.

Mailhot, J., et al. (2006), The 15-km version of the Canadian regional forecast system, *Atmos. Ocean*, *44*(2), 133–149.

Mellor, G. L. (2004), *Users' Guide for a Three-Dimensional, Primitive Equation, Numerical Ocean Model*, 42 pp., Princeton Univ. Press, Princeton, N. J.

Mellor, G. L., and A. F. Blumberg (1985), Modeling vertical and horizontal diffusivities with the sigma coordinate system, *Mon. Weather Rev.*, *113*, 1380–1383.

Pellerin, P., H. Ritchie, F. J. Saucier, F. Roy, S. Desjardins, M. Valin, and V. Lee (2004), Impact of a two-way coupling between an atmospheric and ocean-Ice model over the Gulf of St. Lawrence, *Mon. Weather Rev.*, *132*, 1379–1398.

Rao, Y. R., and C. R. Murthy (2001), Coastal boundary layer characteristics during summer stratification in Lake Ontario, *J. Phys. Oceanogr.*, *31*, 1088–1104.

Saulesleja, A. (1986), *Great Lakes Climatological Atlas*, Cat. En56-70, pp. 36–37, Can. Gov. Publ. Cent. Supply and Serv. Can., Ottawa.

Saylor, J. H., et al. (1981), Water movements, in *IFYGL-International Field Year on the Great Lakes*, edited by E. J. Aubert and T. L. Richards, pp. 7–32, Great Lakes Environ. Res. Lab., Ann Arbor, Mich.

Schertzer, W. M. (1987), Heat balance and heat storage estimates for Lake Erie, 1967 to 1982, *J. Great Lakes Res.*, *13*, 454–467.

Scott, R. W., and F. A. Huff (1996), Impacts of the Great Lakes on regional climate conditions, *J. Great Lakes Res.*, *22*, 845–863.

Segal, M., R. W. Arritt, J. Shen, C. Anderson, and M. Leuthold (1997), On the clearing of cumulus clouds downwind from lakes, *Mon. Weather. Rev.*, *125*, 639–646.

Sheng, J., and Y. R. Rao (2006), Circulation and thermal structure in Lake Huron and Georgian Bay: Application of a nested-grid hydrodynamic model, *Cont. Shelf Res.*, *26*, 1496–1518.

Simons, T. J. (1974), Verification of numerical models of Lake Ontario, part 1: Circulation in spring and summer, *J. Phys. Oceanogr.*, *4*, 501–523.

Simons, T. J. (1975), Verification of numerical models of Lake Ontario, Part 2: Stratified circulations and temperature changes, *J. Phys. Oceanogr.*, *5*, 98–110.

Song, Y., F. H. M. Semazzi, L. Xie, and L. J. Ogallo (2004), A coupled regional climate model for the Lake Victoria Basin of East Africa, *Int. J. Climatol.*, *24*, 57–75.

A. Huang and Y. R. Rao, NWRI, Water Science and Technology Directorate, Environment Canada, 867 Lakeshore Rd., Burlington, ON L7R 4A6, Canada. (ram.yerubandi@ec.gc.ca)

Y. Lu, Department of Fisheries and Oceans, Bedford Institute of Oceanography, 1 Challenger Dr., Dartmouth, NS B2Y 4A2, Canada.